Use of a Discrete Mesoscopic Finite Element Approach Implemented in Abaqus/Explicit to Investigate the Bending and Folding of Fiber-Reinforced Composite Materials during the Manufacturing Process

L. Dangora, J. Sherwood, C. Mitchell, and J. Gorczyca

Department of Mechanical Engineering, University of Massachusetts, Lowell
One University Ave., Lowell, MA 01854, USA

***Abstract**: During the manufacturing of fabric-reinforced composite parts using a matched-die compression molding process or resin transfer molding, the fabric may experience local in-plane compressive loads that cause out-of-plane deformations. The waves that form from such out-of-plane motion can result in resin-rich pockets (during the infusion stage of a dry fabric) or the waves may be forced down into a fold by the tooling. Such defects can compromise the structural integrity of the formed composite part. Therefore, it is valuable to have a simulation tool that can accurately represent the fabric bending properties and predict the locations where waves or folds are likely to form as a result of the manufacturing process. A hybrid finite element model used with a discrete mesoscopic approach is implemented in Abaqus/Explicit to capture the behavior of continuous fiber-reinforced fabrics where the tows are represented by beam elements and the shear behavior is accounted for using shells. User-defined material subroutines describe the mechanical behavior of the beam and shell elements for their respective contributions to the overall fabric behavior. Simulations are used to demonstrate the ability of the modeling approach to predict the amplitude and curvature of out-of-plane waves. A comparison of the simulation results to the experimental data shows the finite element model accurately captures this phenomenon. An additional model is presented to demonstrate the capability of the simulation tool to capture fabric folding.*

***Keywords**: Bending, Composite, Compression, Defects, Fabric, Fiber-Reinforced, Folding, Manufacturing, Out-of-Plane, Processing, Textile, Waves*

1. Introduction

Composite materials have many characteristics that make them favorable for manufacturing in a wide variety of industries including aerospace, automotive, construction, marine, and wind energy (Mazumdar, 2012). For such applications, it is often useful to have a simulation of the manufacturing processes that can be used as a design tool to visualize the effect that processing alterations have on the formed composite part. This approach is less expensive, less time consuming, and more economically friendly than a design-build-test regiment. The finite element method is very amenable to the development of such a simulation tool for fiber-reinforced composites because it can account for the mechanical behavior of the fabric and the complex boundary conditions experienced during manufacturing. A simulation tool that provides orientation information of fabric constituents throughout the manufacturing process can: (1) produce a full-field prediction of the fiber compressive forces, (2) identify localized buckling locations, and (3) track progression of out-of-plane defects. The model results can then be used to make modifications to the tooling and processing conditions to inhibit the onset of out-of-plane defects and thereby prevent the formation of wrinkles or folds. Ultimately, this simulation tool will result in improved structural integrity of the cured composite.

2. Background

2.1 Composite Manufacturing

During the thermostamping of fiber-reinforced composite parts, processing conditions can lead to material instabilities that result in buckling of the fabric. Traditionally, parametric studies are performed to investigate and isolate the respective effects of processing parameters. Once the effects of each factor are well understood, the processing conditions can be adjusted to fabricate defect-free composite parts (Bhattacharyya, 1997). For example, in the thermostamping process (Figure 1a) changes in the pressure applied to the binder (Figure 1b) or the size of the fabric blank (Figure 1c) can eliminate the presence of wrinkles.

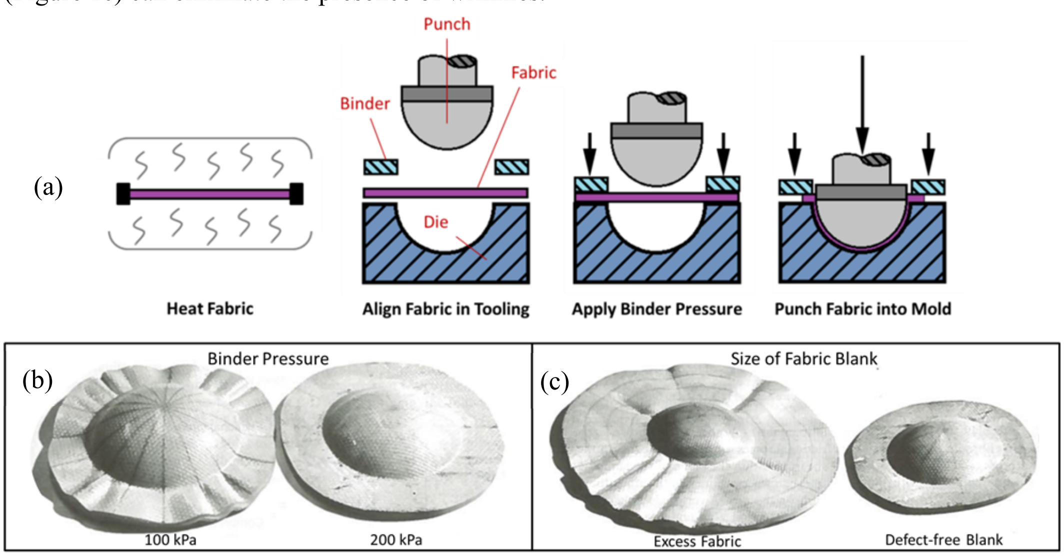

Figure 1. (a) Schematic of the thermostamping process and the effect of (b) binder pressure and (c) blank size on the formation of out of plane defects (Bhattacharyya, 1997)

Another common processing technique prone to fabric waves and buckling is open mold manufacturing in which the dry fabric is laid in the mold by hand, resin is subsequently applied, and vacuum is pulled to promote impregnation of the tows. With angled geometry (Figure 2a), locally high pressures can cause increased resin flow to the outer radii, thereby forcing fibers to collect at the inner radii. This phenomenon, known as matrix migration, will result in resin-rich pockets in the cured composite part as shown in Figure 2b. Additionally, as the resin begins to cure, the inter-ply slippage is inhibited. As a result, the fabric layers are not able to slide relative to each other which ultimately can cause buckling or folding at the inner bend (Figure 2c) (Bhattacharyya, 1997). Matrix migration and fiber buckling can be prevented by using a pressure intensifier (Figure 2a) to locally increase the pressure at small radii (Strong, 2007).

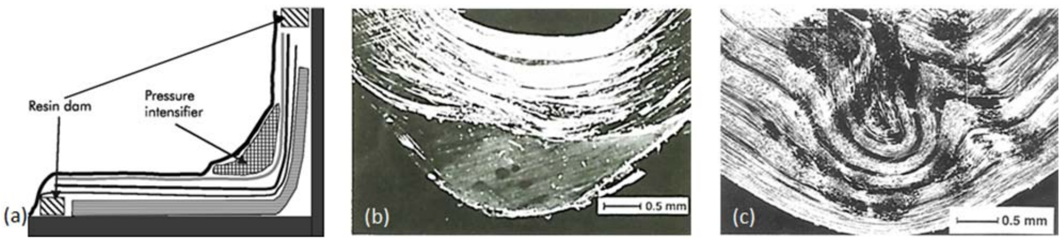

Figure 2. Use of (a) pressure intensifier (Strong, 2007) to reduce (b) matrix migration and (c) fiber buckling (Bhattacharyya, 1997) at the angled geometry during vacuum bagging

2.2 Finite Element Approach

Time, money, and effort can be spared by using a credible simulation tool in which processing parameters and tooling geometry are easily varied to understand their effects on the final morphology and structure of the cured composite (Bhattacharyya, 1997). There are various commercial software applications that have capabilities to perform draping simulations, but these products use a kinematic analysis to predict the progressive blank displacement and do not account for the mechanical behavior of the fabric. Such geometric approaches accommodate only shear deformation of the textile as the mesh grid is mapped to a new surface geometry by means of a "fishnet" algorithm (Borouchaki, 2003). While geometric approaches are fast and efficient, they do not consider the static boundary conditions of the manufacturing process or the mechanical properties of the material (Borouchaki, 2003). As illustrated in Figure 1b, the boundary conditions applied by a binder in the thermoforming process can have a significant effect on the out-of-plane deformations. Additionally, because only in-plane shear deformation is considered by these geometric models, out-of-plane deformations cannot be captured. Though a mechanical analysis using the finite element method is more computationally taxing and may consume more cpu time than a purely geometric model, a mechanical analysis is preferable to achieve high-quality results that can provide insight into the detection, location, and magnitude of defects resulting from part manufacturing.

The finite element method is a mechanical analysis that can be used to simulate the forming of fiber-reinforced composites. With the ability to model the fabrication of composite parts, processing parameters and tooling geometry can be varied in a computer-generated analysis to investigate how variation in the manufacturing conditions effect part quality. For this reason, there is increasing industry interest in the simulation of composite manufacturing processes, and it is desirable to have a simplistic modeling approach that can be easily integrated into commercially available finite element packages.

Modeling the fabric reinforcement can be challenging due to the multi-scale complexity of the fiber interactions. For this research, modeling of the fabric is accomplished at a mesoscopic scale using a discrete approach developed by Jauffrès *et al.* (2010) that employs a hypoelastic element description with an explicit formulation. An explicit solver, chosen for its computational efficiency and robust contact algorithms, was determined to be more amenable to forming simulations than implicit solvers (Jauffrès, 2010).

This modeling technique has been applied to a variety of fabric architectures including woven and non-crimp fabrics (plain-weave and twill-weave, prepreg and stitched). The fabric constituents are modeled using conventional elements present in commercial finite element packages. Linear beam elements are used to incorporate the tensile properties of the tows/roving while shell elements define the shear properties of the fabric. For example, a plain-wave fabric like the one shown in Figure 3 is discretized into a mixed-mesh grid where the unit cell consists of four beam elements and one shell element. The two parallel beam elements on the horizontal carry the properties of the weft tows, and the two parallel beam elements on the vertical embody the warp-tow properties. The shell element has no tensile properties and is only allowed to deform by shearing. Using this modeling technique, the simulation is able to capture the changing orientation of the fabric tows throughout the manufacturing process.

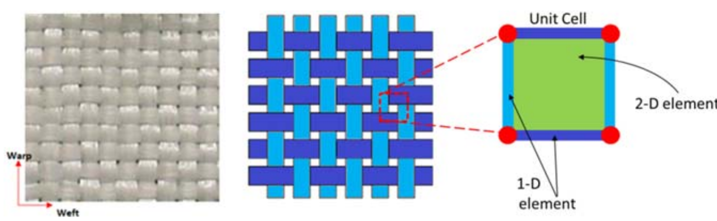

Figure 3. Plain-weave Twintex® fabric and schematic of finite element unit cell

3. Material Characterization

To have a credible simulation tool, the material properties of the fiber reinforcement must be known and properly represented in the finite element model. As demonstrated by the research of Boisse *et al.* (2011), it is critical to account for tensile, shear, and bending behavior of the fabric reinforcement in composite forming applications. Illustrated in in Figure 4a, use of tensile properties alone can simulate the draw-in of fabric and the unsymmetrical deformation of an unbalanced textile, but tensile properties alone cannot predict the onset or progression of out-of-plane defects. Once the locking angle is reached from shear deformation, the fabric is forced to displace out-of-plane. As such, small wrinkling is observed (Figure 4b) when shear properties are integrated into the model. However, the amplitudes and frequencies of the waves generated are not representative of the physical defects seen in Figure 4d. When all three parameters (tensile, shear, and bending) are included, the finite element model approximates deformation seen in the experiment, (see Figure 4c). Boisse *et al.* (2011) results as illustrated in Figure 4 demonstrate the need to fully characterize and incorporate the material properties of the fabric.

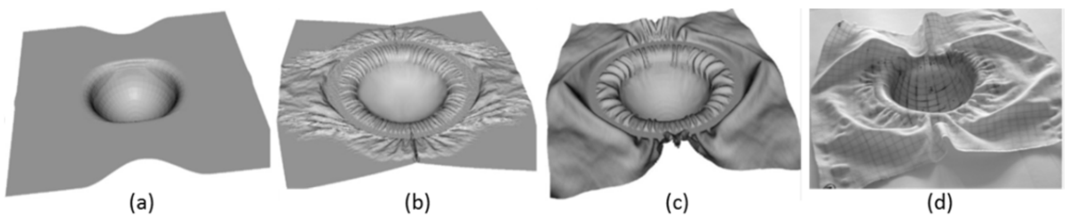

Figure 4. Forming simulation considering (a) tensile properties only, (b) tensile and shear properties, and (c) tensile, shear, and bending properties compared with (d) an experimental part (Boisse, 2011)

Several tests are performed to characterize the mechanical behavior of the fabric in bending, tension and shear. Additional characterization can be performed to identify the frictional behavior of the material in fabric-fabric interaction and fabric-tooling interaction. The measured material properties can then be directly integrated into the Abaqus/Explicit finite element model using user-defined subroutines for material (VUMAT) and friction (VFRIC) behaviors (Fetfatsidis *et al*., 2013).

The bending stiffness of the fabric can be determined following the methods developed by Soteropoulos *et al*. (2011). An initial analysis of the bending stiffness was performed using a vertical cantilever setup (Figure 5a). Still images were taken at tip displacements of 2.54 cm (1 in.) and 5.08 cm (2 in.). The masses required to achieve these displacements were weighed and recorded. Then, the images were analyzed digitally using ImageJ to quantify the deformed shape of the cantilever sample. A finite element model was created to replicate the experiment using a nonlinear beam general section. The bending stiffness of the beam element was varied until the deformed cantilever curvature, and the applied tip force matched what was seen in the experiment. Once the bending stiffness was determined from this iterative approach for the 2.54-cm (1-in.) tip displacement, that same bending stiffness value was used in a model simulating the 5.08-cm (2-in.) displacement. The force and curvature resulting from this second model were compared with experimental data to confirm that the bending stiffness was properly represented (Soteropoulos *et al*., 2011).

Further affirmation that the bending stiffness was properly characterized was accomplished using a different test configuration in which the fabric is axially compressed, as shown in Figure 5b. For this amplitude test, the sample from the cantilever configuration was laid flat and compressed to half of its original length, causing the sample to buckle. As before, a picture was taken of the deformed shape and analyzed in ImageJ to quantify the curvature and amplitude. Using the bending stiffness previously determined, a finite element model was created to replicate the amplitude test. The simulated and experimental results were compared to confirm the bending stiffness was properly characterized.

The material was additionally characterized for tensile stiffness and shear stiffness. The tensile properties of the tows are determined in accordance with ASTM Standard D2256/D2256M-10ε1. In accordance with the methods and calculations outlined by Lussier (2002), the in-plane shear properties of the fabric were determined using a trellis-frame test, also known as the picture-frame test and shear-frame test.

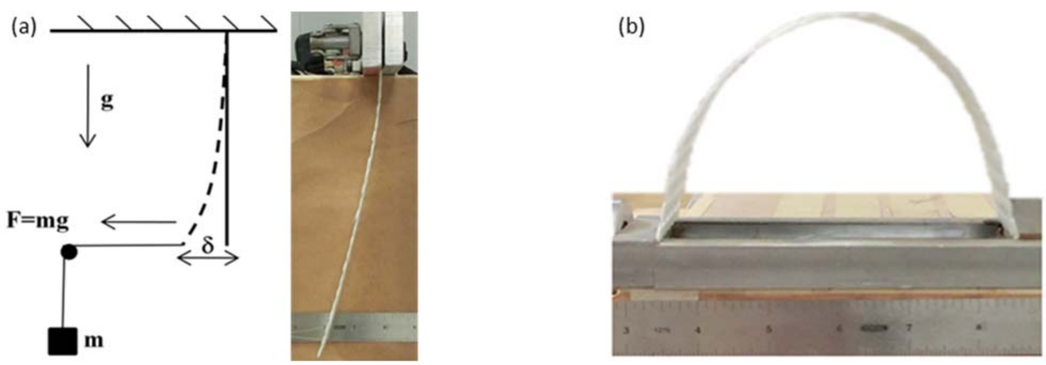

Figure 5. (a) Cantilever and (b) amplitude tests to determine bending stiffness

4. Results and Discussion

A preliminary finite element model was generated in Abaqus/CAE and run in Abaqus/Explicit to explore the capability of the simulation tool to capture a fabric folding over itself. The model was created using material properties for a plain-weave E-Glass fabric with a geometry of 75-mm (2.95-in.) long by 10 tows across. The fiber tows were given a rectangular profile of 6 mm by 1 mm (0.24 in. by 0.04 in.). The left end of the part was pinned, and the right end was displaced axially in a compressive manner at a rate of 20 mm/s (0.79 in/s). Two parallel plates were modeled so the fabric rested on the bottom plate and the top plate moved at a rate of 5 mm/s (0.20 in/s) to close the gap, thereby compressing the fabric from a second direction. The model results, captured in the still images of Figure 6, show the initiation of an out-of-plane wave that progressed to multiple amplitudes. The fabric in the simulation eventually begins to travel underneath a wave which then evolves into a fold. This simulation was purely an academic exercise to explore the capability of the finite element model to capture the phenomenon of fabric folding.

The results confirm that the finite element package in conjunction with the discrete mesoscopic modeling approach is able to predict the onset of out-of-plane deformations and track their progression to form waves and folds. This initial exercise prompted the development of a controlled experimental configuration that can produce out-of-plane defects to assess the predictive capabilities of the modeling approach for wave and fold onset and growth.

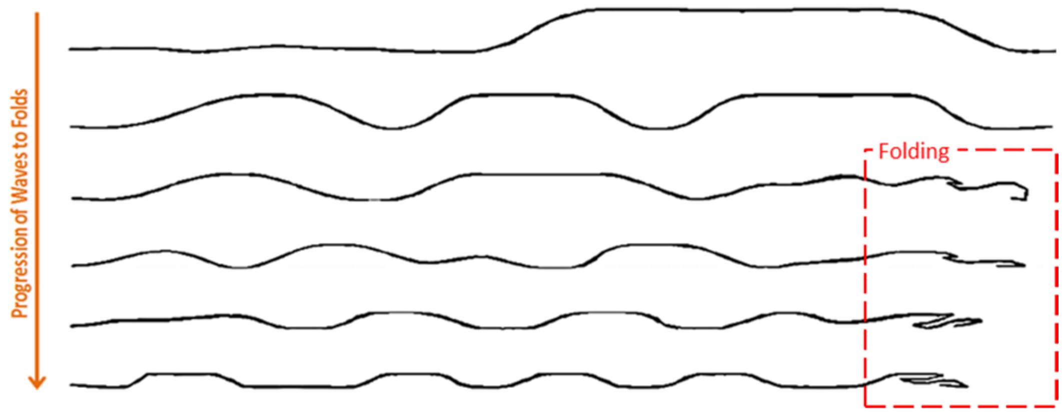

Figure 6. Progression of waves to fabric folds during a compression simulation

4.1 Experimental Configuration

An experimental configuration was designed to produce out-of-plane deformation of a fabric strip. A schematic of the setup and a picture of the fixture during testing are shown in Figure 7. The test fixture can accommodate a maximum sample size of 25.4 cm by 5.08 cm (10 in. by 2 in.). A single layer of the fabric was cut to the maximum size and laid flat in the fixture, placed between two endplates. A piece of Plexiglas extended over the tops of the endplates to create a border parallel to the surface of the undeformed fabric sample. One of the endplates was held stationary while the other moved steadily along a threaded rod with the precision of a micrometer.

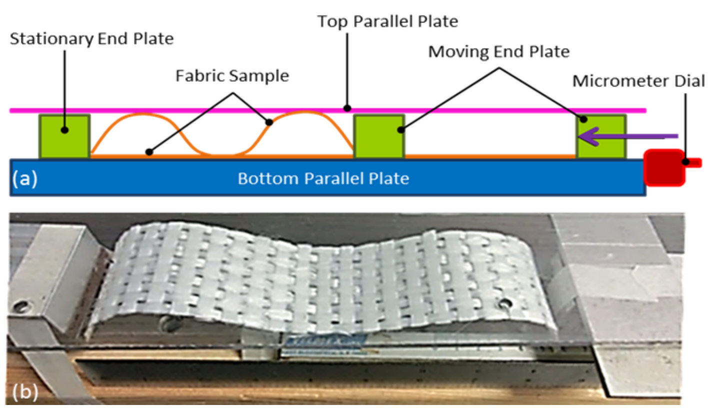

Figure 7. Double compression (a) schematic and (b) experimental configuration

The purpose of this fixture was to produce out-of-plane waves by compressing the fabric from two directions: along the axis of the fibers and normal to the fabric face. Initially, the sample was compressed by axial force only. Once the sample buckled out-of-plane and the wave height exceeded 2.54 cm (1 in.), the fabric was compressed between the bottom surface and the Plexiglas on top. A camera was used to record video of the test and individual frames were extracted to compare with the simulated results of the finite element model.

4.2 Finite Element Model

The fabric tows are represented in the finite element model by linear beam elements. Several modeling options were available in the pre-processor to assign cross-sectional areas to the beams. Because the tows of the fabric were comprised of cylindrical fiber bundles, one common representation of the cross-section was a circular area, as shown in Figure 8a. While the tows were initially formed in a round bundle, when woven into a fabric they tend to flatten out into a rectangular or oblong profile, (see Figure 8b). The third option considered was using a beam general section as illustrated in Figure 8c.

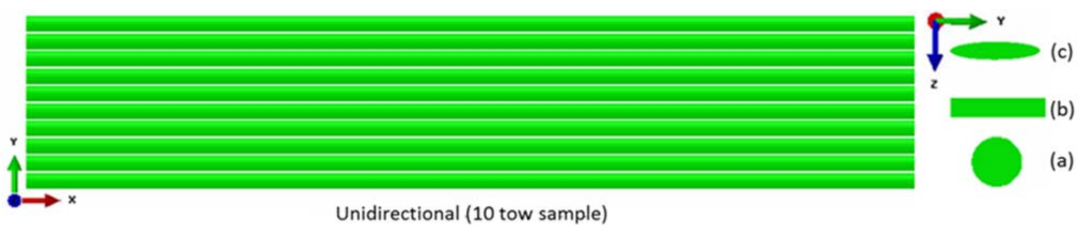

Figure 8. A 10-tow unidirectional fabric sample modeled with (a) circular library section, (b) rectangular library section, and (c) beam general section

The cantilever and amplitude experiments of Figure 5 were recreated in Abaqus/CAE for an E-Glass/Polypropylene Twintex® fabric to determine the sensitivity of cross-sectional modeling approximations on the bending behavior. Four simulations were run for each of the two test configurations shown in Figure 5. Models were created using the circular beam library section (Figure 8a) and the rectangular beam library section (Figure 8b). Two additional models were generated using the beam general section (Figure 8c) with properties calculated in two different manners consistent with the cross-sectional geometries of Figure 8a and Figure 8b. The results of the four models were compared to experimental data for the amplitude and cantilever tests (Figure 9). While slight differences can be seen among the results, reasonable agreement was noted, which suggested any of the cross-sectional shapes were sufficient for modeling the fabric tow cross-sectional area. Also, the data confirmed that a generic profile from the beam cross-section library can be used in conjunction with the user-defined material subroutine (VUMAT) to achieve an appropriate representation of the fabric's actual bending behavior. Therefore, it was unnecessary to calculate and define a specific beam general section when this beam definition performs comparably to those definitions available in the built-in cross-section library.

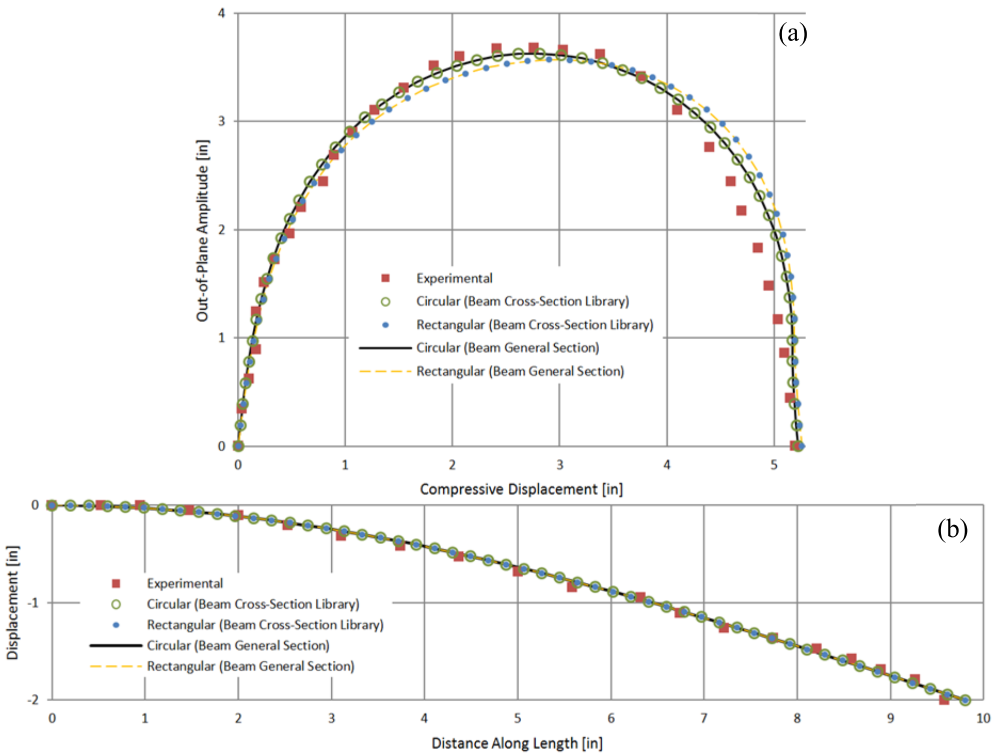

Figure 9. (a) Amplitude and (b) cantilever cross-section comparison

4.3 Comparison

A finite element model was created to replicate the double-compression test shown in Figure 7. Because the sample sizes were relatively small, the fabric mesh was modeled on a one-to-one scale with the test specimen (Figure 3). One endplate was assigned a fixed boundary condition while the other was displaced 76 mm (3 in.) to axially compress the fabric. The results of the analysis were compared to experimental images for two different fabric architectures.

A Twintex® fabric with plain-weave architecture made of E-Glass and comingled polypropylene fibers was tested. Still images taken during the experiment were compared with finite element simulation results, (see Figure 10). The FEA model was able to predict the evolution of the fabric's compressive deformation with reasonable accuracy. In the initial stages, the asymmetry of the wave formation was captured (Figure 10a through Figure 10c) and the progression to two wave amplitudes was also observed (Figure 10d through Figure 10h). The model simulated the profile and slight asymmetry of the final deformed state of the fabric sample.

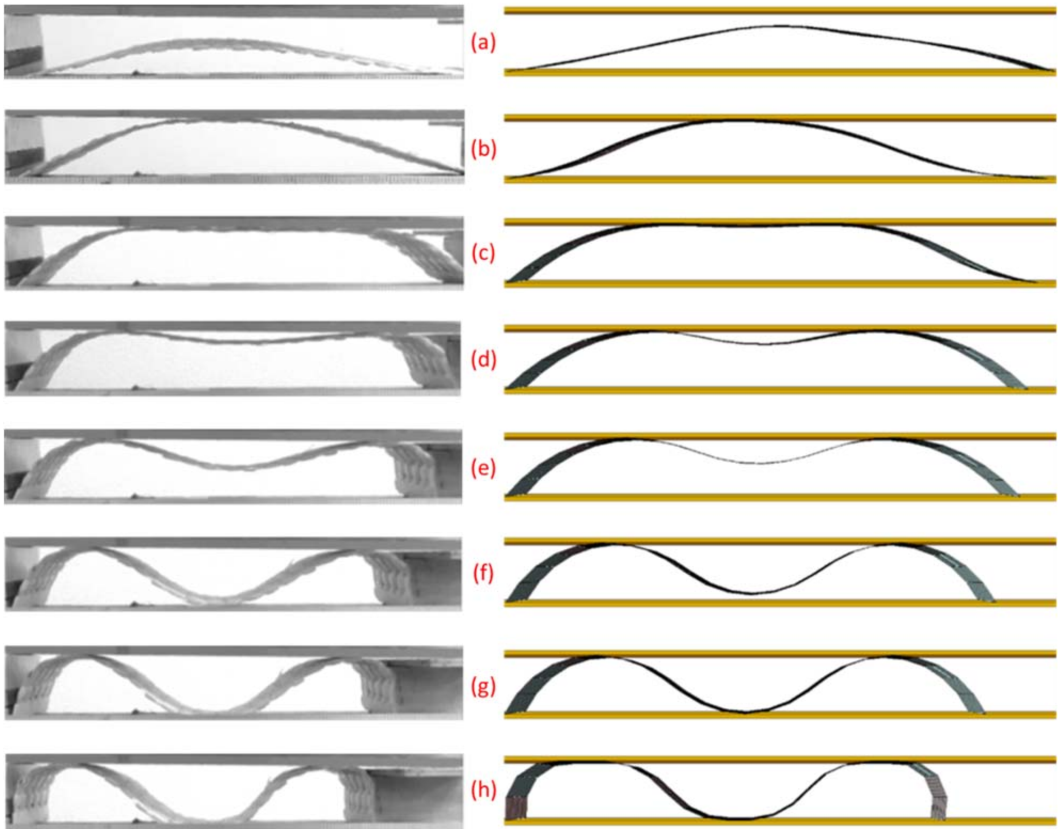

Figure 10. Comparison of experimental and simulated double compression specimen for a plain-weave comingled E-Glass/Polypropylene Twintex® fabric

A second fabric architecture was investigated using Vectorply E-LT 2900. This stitched bias biaxial E-Glass fabric was compressed in the warp direction. The experimental and finite element results are presented in Figure 11. Good agreement was seen in the initial deformation stages (Figure 11a through Figure 11e). In the later stages of deformation (Figure 11f through Figure 11h), there was some discrepancy between the model and experiment. The test images show a more pointed amplitude where the fabric contacts with the top Plexiglas surface whereas the simulated profile shows a flatter contact. Also, there were discrepancies at the left boundary, but these differences can be explained to be due to the use of masking tape in the experimental testing. The tape was needed to apply a uniform force to the fabric sample, but it had a stiffening effect at the edges of the strip. However, the asymmetry of the deformation as well as the initiation site of a fabric fold at the right end of the sample were still captured as seen in Figure 11h.

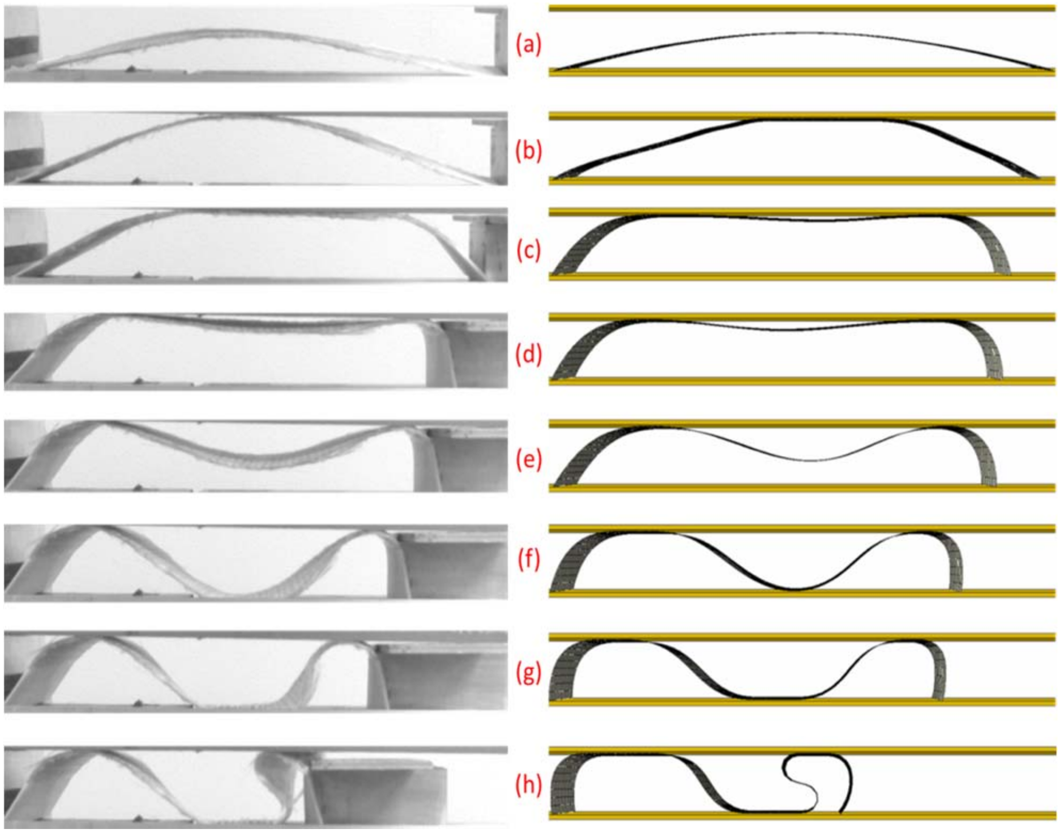

Figure 11. Comparison of experimental and simulated double compression specimen for a stitched bias biaxial E-Glass fabric

5. Conclusions

The fabric model as implemented in Abaqus/Explicit is amenable to creating a credible simulation tool to investigate the composite manufacturing process and to aid in design changes and modifications to processing conditions to produce a defect-free final part. To predict the onset and progression of out-of-plane defects, it is critical to fully characterize the mechanical behavior of the fabric, including tensile, bending and shear stiffness. Experimental testing is performed to determine the fabric's material properties which are directly incorporated into the Abaqus model with a user-defined material subroutine (VUMAT). The discrete mesoscopic modeling approach is able to capture the compressive response of the fabric as wrinkles, waves, and folds are produced. An experimental setup was created to generate out-of-plane deformations that can be compared to the modeling results, and good agreement was noted between the finite element predictions and the physical phenomenon.

6. References

1. Bhattacharyya, D., *Composite Sheet Forming*, Amsterdam, New York: Elsevier, 1997.
2. Boisse, P., Hamila, N., Helenon, F., Hagege, B., Cao, J., "Different Approaches for Woven Composite Reinforcement Forming Simulation," International Journal of Material Forming 1:21–29, 2008
3. Boisse, P., Hamila, N., Vidal-Salle, E., Dumont, F., "Simulation of wrinkling during textile composite reinforcement forming. Influence of tensile, in-plane shear and bending stiffnesses," Composites Science and Technology 71, p. 683-692, 2011.
4. Borouchaki, H., Cherouat, A., "Geometrical Draping of Composite Fabrics," C.R. Mecanique 331. p. 437-442, 2003.
5. Fetfatsidis K, A., Gamache L, M., Gorczyca J, L., Sherwood J, A., Jauffres, D., & Chen, J., "Design of an Apparatus for Measuring Tool/Fabric and Fabric/Fabric Friction of Woven-Fabric Composites During the Thermostamping Process," International Journal Of Material Forming, 2013.
6. Hoa, S. V., *Principles of the Manufacturing of Composite Materials*, Lancaster, PA: DEStech Publications, 2009.
7. Hyer, M., *Stress Analysis of Fiber-Reinforced Composite Materials*, Lancaster, PA: DEStech Publications, 2008.
8. Jauffrès, D., Sherwood, J.A., Morris, C.D., Chen, J., "Discrete Mesoscopic Modeling for the Simulation of Woven-Fabric Reinforcement Forming", International Journal of Material Forming, Vol. 3, Suppl. 2, p. 1205-1216, 2010.
9. Lussier D. *Shear Characterization of Textile Composite Formability*, Master's Thesis, University of Massachusetts Lowell: Department of Mechanical Engineering, 2002.
10. Mazumdar, S., "Growth Opportunities: Materials Innovation Will Drive Composites Usage to New Heights." Composites World. High-Performance Composites, 1 May 2012.
11. Soteropoulos, D., Fetfatsidis, K., Sherwood, J.A., Langworthy, J., "Digital Method of Analyzing the Bending Stiffness of Non-Crimp Fabrics," AIP Conference Proceedings, Vol. 1353 Issue 1, p. 913-917, 2011.
12. Strong, A. B., *Fundamentals of Composites Manufacturing: Materials, Methods and Applications*, Dearborn, MI: Society of Manufacturing Engineers, 2007.
13. ASTM Standard D2256/D2256M – 10ε1, "Standard Test Method for Tensile Properties of Yarns by the Single-Strand Method," ASTM International, West Conshohocken, PA, DOI: 10.1520/ D2256_D2256M-10E01, www.astm.org, 2010.